Journal of Innovative Materials in Extreme Conditions
2021
Volume 2
Issue 2

EFFECT OF PROCESSING PARAMETERS ON Ti_3Al-BASED ALLOY HIGH-TEMPERATURE CYCLIC OXIDATION KINETICS

Ivana Cvijović-Alagić*, Milan T. Jovanović
Center of Excellence "CEXTREME LAB", Vinča Institute of Nuclear Sciences - National Institute of the Republic of Serbia, University of Belgrade, Mike Petrovića Alasa 12-14, 11001 Belgrade, Serbia
Corresponding author: ivanac@vinca.rs*

Abstract: *Efficient exploitation of the industrial components at elevated temperatures and in aggressive environments is demanded in modern industrial production. The Ti_3Al-based alloys are proposed as materials that can meet these demands since it is determined that improved high-temperature corrosion resistance of industrial construction materials is often more significant for industrial exploitation than the improvement of their mechanical properties. Therefore, the aim of the present research was to determine the effect of various parameters, i.e. initial microstructure and high-temperature processing conditions, on the cyclic oxidation kinetics of the Ti_3Al-based alloy with the Ti-24Al-11Nb (at.%) composition. Cyclic oxidation tests were conducted in air at 600 and 900 ^oC. The oxidation process was monitored up to 120 h by recording mass gain data as a function of time to define the kinetic models. Examination of alloy microstructure and alloy degradation during the cyclic oxidation was undertaken using light microscopy (LM), scanning electron microscopy (SEM), energy dispersive spectroscopy (EDS), and X-ray diffraction (XRD). Alloy hot-rolled at 1050 ^oC and hot-rolled alloy subsequently thermally treated at 1200 ^oC were examined before and after cyclic high-temperature oxidation. Obtained results indicated that the initial alloy microstructure has a significant influence on its high-temperature oxidation behavior. Namely, hot-rolled alloy thermally treated at 1200 ^oC with a higher volume fraction of the β phase in the microstructure shows improved oxidation resistance compared to the alloy only hot-rolled at 1050 ^oC. An increase in oxidation temperature caused the progress in alloy degradation. In contrast to the compact external layer formed at the alloy surface after cyclic oxidation at 600 ^oC, during cyclic oxidation at 900 ^oC formation of a multi-layer scale was observed. The main products of oxidation are Al_2O_3 and TiO_2. Kinetic models of the Ti-24Al-11Nb (at.%) alloy cyclic oxidation at 600 ^oC and 900 ^oC in the air are defined with linear and parabolic oxidation curves for most of the examined conditions.*

Keywords**:** *Ti-24Al-11Nb alloy, thermo-mechanical processing, phase distribution, cyclic oxidation, external scale, internal diffusion zone, kinetic model*

1. Introduction

Production of more durable structural components, which can withstand exploitation at extreme temperatures and in extremely corrosive environments without degradation and failure, is crucial for modern industrial advancements [1, 2]. Obtainment of materials resistant to high-temperature oxidative degradation is extremely important in automotive and aviation applications where structural components are subjected to extreme temperature variations in the highly-corrosive gas atmosphere. Moreover, structural components produced for these applications should be characterized by low density and exceptional mechanical properties to fulfill strict demands regarding low fuel consumption and low air pollutant emission. These challenges led to the intensification of research in the field of intermetallic titanium-based materials. Special attention is directed to the development of titanium aluminides, such as Ti_3Al-based alloys, as these materials show improved mechanical properties at elevated temperatures, good dimension stability, lower density, and higher oxidative durability than nickel- and iron-based superalloys and can be used for the production of turbines, engines, and gas exhaust systems [3-6].

Conventional Ti-based alloys were for decades materials of choice for the construction of machine parts with improved work efficiency. However, these alloys showed poor mechanical properties at temperatures higher than 600 °C and poor creep and fatigue resistance in demanding

exploitation conditions. Moreover, early failure of machine parts at elevated temperatures is often caused by the surface formation of a brittle oxide layer. Recent developments in this field indicated the Ti_3Al-based alloys as materials suitable for exploitation in extreme industrial conditions where an increase of the material's high-temperature oxidation resistance is more important than an increase of its creep and fatigue resistance [7-14]. Additional alloying of binary titanium aluminides with β-stabilizing elements, such as Nb, V, and Mo, showed beneficial effects on their room-temperature ductility and oxidation resistance due to their β-phase stabilizing effect [15, 16]. However, additional alloying of titanium aluminides with ternary elements is not sufficient to ensure their exceptional oxidation resistance at elevated temperatures and should be complemented with other methods, such as thermo-mechanical processing [14, 16-20]. Namely, α_2-Ti_3Al-based alloys can not be used as single-phase materials due to their poor room-temperature ductility [21]. Enhanced ductility is attained via duplex α_2 and β phase microstructure obtained by selection of appropriate alloy chemical composition and/or thermal treatment. Furthermore, an increase of the β phase content in the microstructure of these alloys contributes to the increase of their oxidation stability at elevated temperatures.

Therefore, the scope of the present study was to investigate the influence of processing parameters on the high-temperature oxidation behavior of the Ti_3Al-based alloy with special emphasis on oxidation kinetics.

2. Experimental Procedures

For the present investigation, the Ti_3Al-based alloy with the Ti-24Al-11Nb (at.%) composition was selected. The investigated alloy was supplied in the form of hot-rolled sheets with a thickness of 0.5 mm. Hot-rolling of the alloy was performed at 1050 °C in the two-phase (α_2+β) field. From the hot-rolled alloy sheets, samples with a size of 15 × 15 mm^2 were cut. One group of samples was additionally subjected to annealing at 1200 °C in the β-phase field and subsequent water quenching to induce microstructural modifications and examine the influence of the alloy phase composition on its high-temperature oxidation kinetics. Detail description of the alloy production and thermo-mechanical processing procedures is given previously [22]. Samples of the alloy hot-rolled at 1050 °C and the hot-rolled alloy thermally treated at 1200 °C were metallographically prepared and ultrasonically cleaned with ethyl alcohol to eliminate any surface contamination.

Alloy samples were subjected to the high-temperature cyclic oxidation in air at 600 °C and 900 °C in five successive cycles. For each oxidation cycle, the samples were oxidized in a tube furnace for 24 h at test temperature and subsequently furnace-cooled down to room temperature. Mass gain, Δm, was measured after each oxidation cycle using the Mettler electronic balance with ±0.0001 g accuracy to determine the mass gain *vs.* oxidation time function and oxidation kinetics parameters.

A Reichert Jung light microscope (LM) was utilized to undertake the microstructural characterization of the alloy hot-rolled at 1050 °C and the hot-rolled alloy thermally treated at 1200 °C. For that purpose, previously metallographically prepared samples were etched in Kroll's reagent that contains 3 ml HF, 6 ml HNO_3 and 91 ml H_2O. Additional identification of the phases present in the alloy microstructure was conducted using a Simens D500 PC automatic x-ray diffractometer (XRD) with CuK_α radiation. The XRD analysis was also used to determine the composition of external scales formed on the sample surface during the high-temperature oxidation process. A JEOL JSM-6460LV scanning electron microscope (SEM) was used for the oxidized samples' cross-sectional analysis and estimation of the oxidation affected zones thickness and morphology, while the elemental composition of the formed oxide scales was determined by energy dispersive spectrometer (EDS) Oxford Instruments INCA X-sight system attached to the SEM.

3. Results and Discussion

Typical duplex microstructure obtained during the hot-rolling of the Ti-24Al-11Nb alloy at 1050 °C and subsequent slow cooling to room temperature is presented in Fig. 1a. The obtained XRD patterns confirmed the already established presence of duplex microstructure, Fig. 1c. The appearance of the diffraction peaks at 34.5°, 38.7°, 58°, 62.5°, and 72° indicate the existence of the α_2-Ti_3Al phase in the microstructure, while the presence of the diffraction peaks at 35.7°, 72.5°, 83.8°, and

94.6° confirm the existence of the β-Ti phase in the microstructure. Quantitative microstructural analysis revealed that the α_2 and β phase are present in approximately equal volume fractions, Fig. 1d. Namely, the volume fraction of α_2-Ti_3Al phase, observed as bright irregularly shaped grains in the LM micrograph present in Fig. 1a, is slightly higher than the volume fraction of β-Ti phase (~5.94 vol.%).

Microstructure of the hot-rolled Ti-24Al-11Nb alloy thermally treated at 1200 °C and subsequently water quenched is presented in Fig. 1b. Rapid cooling from the single-phase field did not prevent the transformation of the high-temperature β phase. Namely, in the dark matrix, shown in Fig. 1b, one can observe the presence of bright elongated platelets appearing inside and at the grain boundaries. The XRD analysis confirmed that these platelets are the α_2-Ti_3Al phase which appeared in the microstructure as a result of the β-Ti phase transformation during the rapid cooling from the thermal treatment temperature, Fig. 1c. Since rapid cooling from the thermal treatment temperature prevented the complete $\beta \rightarrow \alpha_2$ transformation it can be expected that the metastable β-Ti phase is present in the microstructure in higher volume fraction than in the microstructure formed during the slow cooling after the hot-rolling treatment. Quantitative microstructural analysis showed that rapid cooling resulted in the phase distribution that differs from the phase distribution in the hot-rolled alloy microstructure. Namely, the results of the quantitative microstructural analysis showed that the volume fractions of the α_2 and β phase are approximately 40% and 60%, respectively (Fig. 1d).

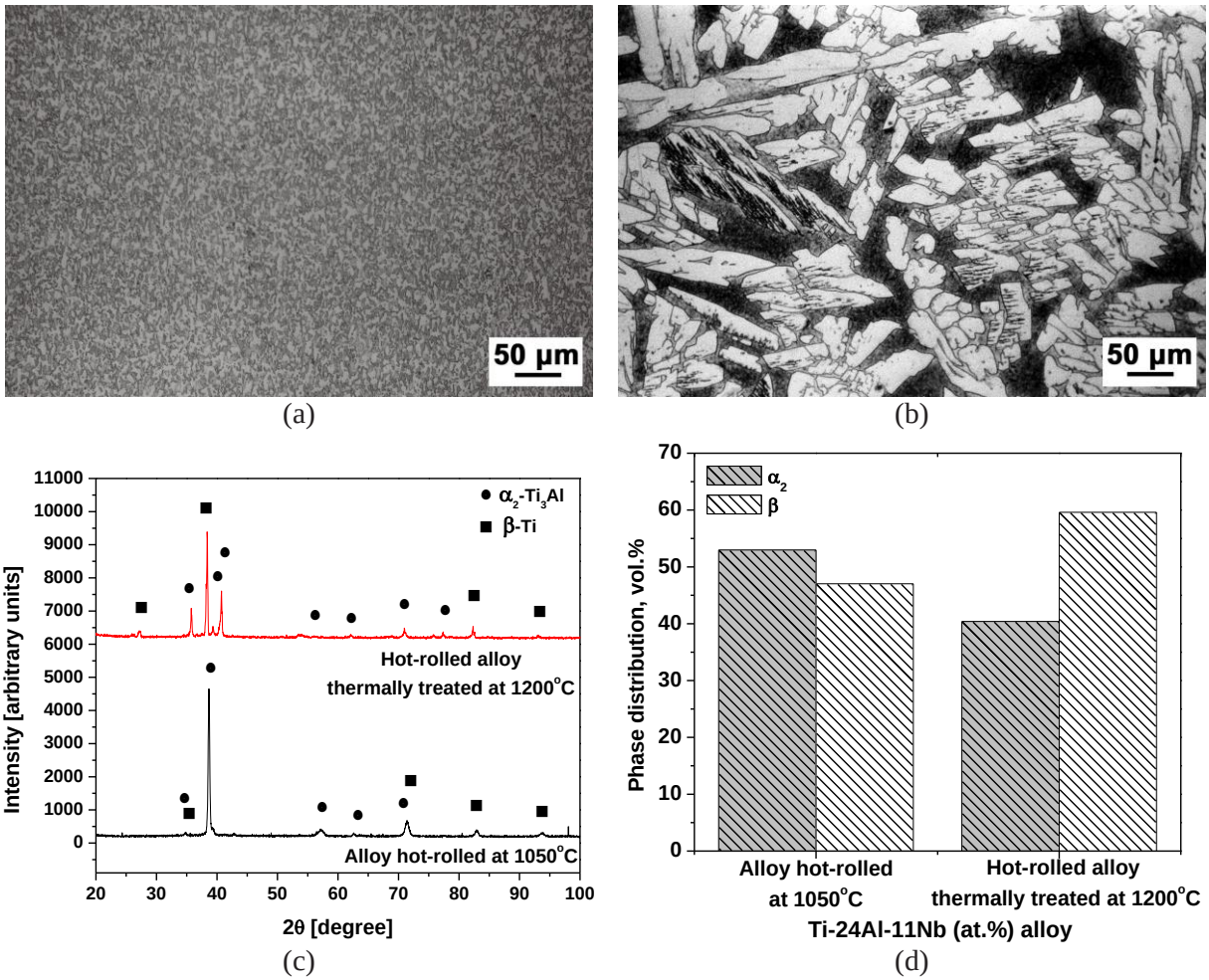

Figure 1. (a,b) LM micrographs of the Ti-24Al-11Nb alloy microstructure obtained (a) during hot-rolling at 1050 °C and (b) subsequent thermal treatment at 1200 °C accompanied with corresponding (c) XRD patterns and (d) phase distribution.

Detail investigations conducted in this study reviled that modification of the Ti-24Al-11Nb alloy microstructure, attained during the thermal treatment at 1200 °C of the hot-rolled alloy, influenced the change in alloy cyclic oxidation mechanism and increased the alloy high-temperature

oxidation resistance. The observed increase of the alloy high-temperature oxidation resistance is determined to be highly dependent on the cyclic oxidation temperature and oxidation duration due to the change of selective oxidation model, morphological characteristics of the externally formed scales, preferential formation of the protective Al_2O_3 oxide particles, and thickness of the internally formed diffusion zone.

Table 1. Effect of processing parameters and oxidation conditions on the Ti-24Al-11Nb alloy surface characteristics.

Alloy processing conditions	**Oxidation temperature [°C]**	**Surface characteristics**	**High-temperature oxidation time [h]**		
			24	**72**	**120**
Alloy hot-rolled at 1050 °C	600	External scale composition	Al_2O_3, AlN	TiO_2, AlN	TiO_2, AlN, Ti_2AlN
		External scale morphology	compact external scale with good adherence to the alloy surface	compact external scale	some cracking of external scale which is detaching from alloy surface
	900	External scale composition	Al_2O_3, TiO_2, Nb, AlN, TiN	Al_2O_3, TiO_2, Nb, AlN, TiN	Al_2O_3, TiO_2, Nb, AlN, TiN
		External scale morphology	formation of two-layered internal diffusion zone and presence of small cracks and pores in three-layered external scale	porous, granular, multi-layered external scale detaching from alloy surface and internal diffusion zone with coarse lamellae	porous multi-layered external scale with big cracks is detaching from alloy surface
Hot-rolled alloy thermally treated at 1200 °C	600	External scale composition	Al_2O_3	Al_2O_3	Al_2O_3, TiO_2, Nb
		External scale morphology	indistinctive oxide layer with locally present oxide particles	local appearance of oxide clusters due to slow oxidation process	incompact external scale susceptible to detachment
	900	External scale composition	Al_2O_3, TiO_2, Nb	Al_2O_3, TiO_2, AlN, Nb	Al_2O_3, TiO_2, AlN, Nb
		External scale morphology	appearance of cracks in multi-layered external scale with variable thickness	appearance of cracks in multi-layered external scale with porous and uncompacted layers	stagnation of oxidation process and appearance of cracks in multi-layered external scale

Results of the SEM/EDS cross-sectional analysis, summarized and presented in Table 1, indicate that higher volume fraction of the β phase in the alloy microstructure caused an increase of the alloy oxidation resistance even at 600 °C due to the preferential formation of the compact external scale composed mainly of protective Al_2O_3 oxide particles contrary to the scale formed at the surface of the alloy processed only by hot-rolling at 1050 °C which is composed mainly of the TiO_2 oxide particles. Namely, except the nitride particles at the surface of the hot-rolled alloy during the later stages of cyclic oxidation at 600 °C the TiO_2 oxide particles are formed and their presence caused the cracking of the externally formed scale. Moreover, a higher volume fraction of the β phase, as a phase which is enriched with Nb, resulted in the higher thermodynamical activity of Al, protective Al_2O_3 oxide particles formation, and Nb diffusion into the externally formed scale. The overall thickness of

the external and internal zones, formed at the surface and in the subsurface regions of the investigated alloy samples, is shown in Fig. 2.

Positive effect of a higher volume fraction of the β phase in the microstructure is even more evident during the cyclic oxidation at 900 °C. Namely, even though the formation of the multi-layered external scale at the surface of the hot-rolled alloy thermally treated at 1200 °C is faster at the beginning of the cyclic oxidation process than in the case of the alloy hot-rolled at 1050 °C, in the later oxidation stages this process significantly decelerates and, as a result, overall external scale thickness is found to be 35% lower for the alloy samples characterized with higher β phase volume fraction, Fig. 2. Furthermore, when the hot-rolled alloy thermally treated at 1200 °C is concerned, it is evident that the oxidation process is taking place only at the alloy surface and that the externally formed layers, although porous and cracked, do not spall from the surface, Table 1. Results of the SEM/EDS analysis, summarized in Table 1, indicate that the multi-layered external scale formed during cyclic oxidation at 900 °C is composed of alternating TiO_2 and Al_2O_3 layers and the mixture of these two oxides.

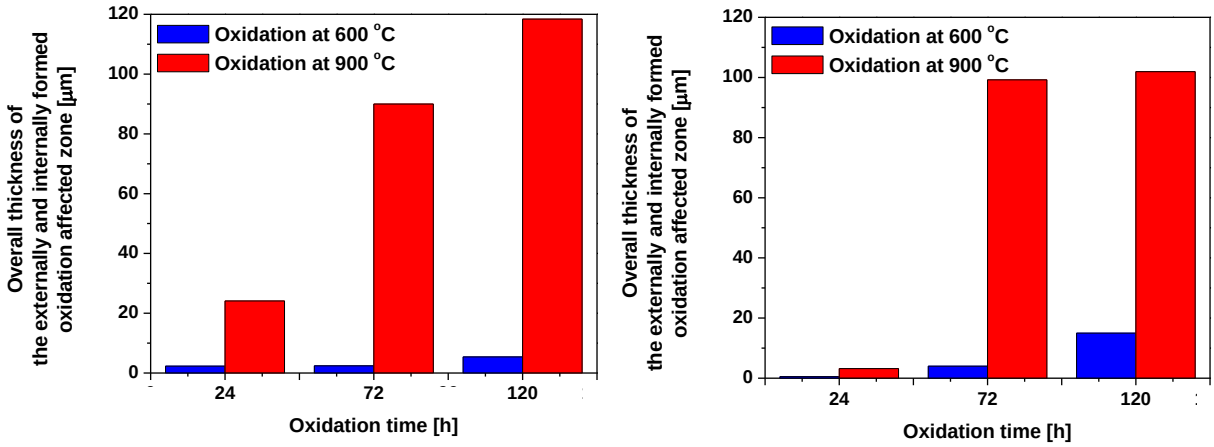

(a) (b)

Figure 2. Effect of cyclic oxidation parameters on the overall thickness of the externally and internally formed oxidation affected zones: (a) alloy hot-rolled at 1050 °C, (b) hot-rolled alloy thermally treated at 1200 °C.

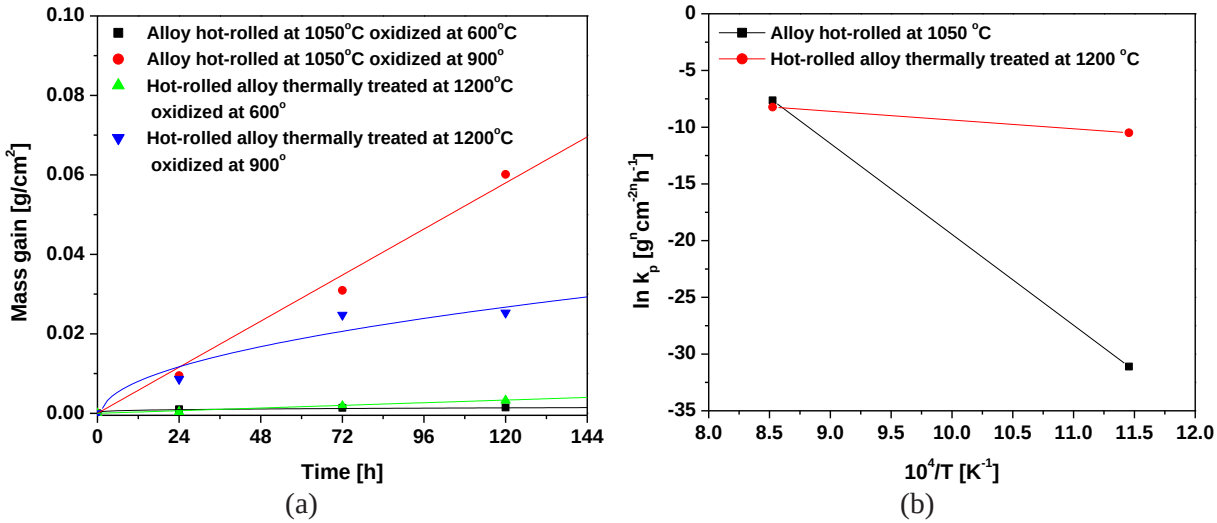

(a) (b)

Figure 3. (a) Mass gain data and (b) Arrhenius plots of oxidation rate constants of the Ti-24Al-11Nb alloy hot-rolled at 1050 °C and hot-rolled alloy thermally treated at 1200 °C.

Detail examination of the Ti-24Al-11Nb alloy behavior during the high-temperature cyclic oxidation showed that modification of the alloy microstructural features induced by the additional thermal treatment at 1200 °C of the hot-rolled alloy significantly improved the investigated alloy

response to gas corrosion degradation at elevated temperatures. Namely, a positive effect of the β phase content increase on the alloy oxidation resistance is additionally confirmed by a significantly lower mass gain recorded for the oxidation process at 900 °C presented in Fig. 3a. However, to define and better understand the oxidation process it is necessary to determine the oxidation kinetic models. Oxidation rate can be defined with different kinetic models determined by designing of the thermogravimetric curves, *i.e.* mass gain variation with time, and by specifying kinetic parameters, *i.e.* rate constant, oxidation rate power exponent, and activation energy. Oxidation rate can be described using the model presented in Eq. (1):

$$(\Delta m)^n = k_p \cdot t \,. \tag{1}$$

where Δm is mass gain per unit surface area, n is oxidation rate power exponent, k_p is oxidation rate constant and t is oxidation time. The following dependence derived from Eq. (1):

$$\log(\Delta m) = \frac{1}{n}\log k_p + \frac{1}{n}\log t \,. \tag{2}$$

Linear regression fitting of *log (Δm) vs. log t* data for all investigated conditions is utilized to evaluate and determine oxidation power exponent and oxidation constant values. According to the data obtained using this method, it can be said that when n=1 then mass gain with time variation is considered to be linear, when n=2 then this variation is considered as parabolic, etc. [23].

Table 2. Effect of processing parameters and oxidation conditions on the Ti-24Al-11Nb alloy oxidation kinetic parameters.

Alloy processing conditions	Oxidation temperature [°C]	Oxidation rate power exponent, n	Oxidation rate constant, k_p [$g^n cm^{-2n} h^{-1}$]
Alloy hot-rolled at 1050 °C	600	4	2.98419×10^{-14}
	900	1	4.99147×10^{-4}
Hot-rolled alloy thermally treated at 1200 °C	600	1	2.77973×10^{-5}
	900	2	6.015×10^{-6}

Isothermal curves, obtained during this study, confirmed better oxidation resistance behavior of the investigated alloy during the oxidation at 600 °C than during the oxidation at 900 °C, irrespective of the alloy processing procedure, Fig. 3a. Namely, results obtained during the mass gain measurements revealed that the linear increase of the mass gain values with cyclic oxidation time is characteristic for the oxidation at 900 °C of the alloy hot-rolled at 1050 °C and oxidation at 600 °C of the hot-rolled alloy thermally treated at 1200 °C. Attained data combined with the surface chemical and morphological analysis results indicate that oxidation of the hot-rolled alloy at 900 °C did not result in the protective surface scales formation and therefore led to the oxidation process intensification. This observation is supported by the SEM/EDS results, presented in Table 1, which reveal that the externally formed multi-layered scale is porous and prone to cracking, detachment and spallation implying the oxidation process acceleration. Moreover, the highest value of the oxidation rate constant, as an indicator of the high oxidation rate, is observed for the oxidation at 900 °C of the alloy hot-rolled at 1050 °C, see Table 2. When oxidation at 600 °C of the hot-rolled alloy thermally treated at 1200 °C is concerned then it can be noted that the linear dependence observed for the alloy oxidative degradation behavior is a consequence of the modification of oxide scale composition with the oxidation time, Tables 1 and 2. Namely, at the beginning of the oxidation process on the alloy surface the incompact protective Al_2O_3 layer is formed, however, during the later oxidation stages the surface layer composition is changed and the amount of undesirable TiO_2 is increasing in the external scale. Cracking and detachment of the newly-formed TiO_2 layer are accelerating the oxidation process, which is confirmed by the moderately high k_p value, Table 2.

An increase of the β phase content in the alloy microstructure, induced by thermal treatment at 1200 °C, showed the significant influence on the oxidation rate reduction during the cyclic

treatment at 900 °C which is evident by the obtainment of the three orders of magnitude lower k_p value than the k_p value obtained for the alloy hot-rolled at 1050 °C under the same oxidizing conditions, Table 2. Lower k_p value and parabolic mass gain *vs.* time dependence (n=2) are caused by the formation of protective Al_2O_3 oxides and change in the oxides forming mode, Tables 1 and 2.

Oxidative degradation of the hot-rolled alloy during the cyclic oxidation at 600 °C can be described by mass gain *vs.* time dependence of fourth-order, Table 2. Since oxidation of the hot-rolled alloy at 900 °C is characterized by linear dependence of the mass gain with time (n=1) it is evident that this process is significantly faster than in the case of the oxidation process conducted at lower temperature and obtained k_p values confirm this finding, Table 2. Change in the kinetic model of the hot-rolled alloy indicates the change in the external scale formation mode from single-layered scale obtained during oxidation at 600 °C to multi-layered scale obtained during oxidation at 900 °C, Tables 1 and 2.

Effect of the cyclic oxidation temperature on the Ti_3Al-based alloy oxidation rate can be determined after the kinetic models were completely defined. Namely, following the Arrhenius law it is possible to define values of activation energies based on the previously defined oxidation rate constants. Oxidation rate constant dependence on the oxidation temperature can be determined according to the Arrhenius equation:

$$k_p = k_o \exp\left(-\frac{E_a}{RT}\right). \quad (3)$$

where k_o is pre-exponential factor, E_a is the activation energy, R is the universal gas constant and T is absolute temperature. However, to completely define the oxidation rate constant, E_a and k_o values must be determined by plotting *ln* k_p *vs. 1/T*. Plots of *ln* k_p as a function of *1/T* for the oxidation of alloy hot-rolled at 1050 °C and hot-rolled alloy thermally treated at 1200 °C are presented in Fig. 3b. Activation energies are determined from the slopes of these plots. The experimentally obtained values of activation energies and pre-exponential constants are presented in Table 3.

Table 3. The Ti-24Al-11Nb alloy oxidation kinetic parameters.

Alloy processing conditions	E_a [KJ/mol]	k_o [$g^n cm^{-2n} h^{-1}$]*
Alloy hot-rolled at 1050 °C	668.0951	2.80755×10^{26}
Hot-rolled alloy thermally treated at 1200 °C	641.1294	0.19055

*n = oxidation rate power exponent

Differences in the experimentally obtained E_a values for the alloy hot-rolled at 1050 °C and the hot-rolled alloy subjected to additional thermal treatment at 1200 °C indicate that the high-temperature cyclic oxidation process is not controlled by the same mechanism. A significant increase in the k_p values showed that alloy oxidation resistance was drastically reduced during exposure to air at 900 °C, especially in the case of the alloy hot-rolled at 1050 °C. However, since oxidation rate is proved to be highly dependent on the alloy phase composition it was found that an increase of the β phase content in the alloy microstructure significantly improved its oxidation resistance at higher exposure temperature, which was confirmed with obtained k_p values.

4. Conclusions

The present research was focused on the effect of processing parameters on the Ti-24Al-11Nb alloy high-temperature cyclic oxidation kinetics and resulting conclusions are summarized as follows:

1. Cyclic oxidation of the Ti-24Al-11Nb alloy at 600 °C and 900 °C in the air for 120 h resulted in external and internal oxidation of the alloy hot-rolled at 1050 °C, as well as the hot-rolled alloy thermally treated at 1200 °C. The initial microstructure of the investigated alloy, *i.e.* volume fractions of the α_2 and β phase in the alloy microstructure, showed a significant influence on the gas corrosion degradation and oxidation kinetics of the Ti_3Al-base alloy. Obtained results confirmed that the β phase is characterized by higher oxidation resistance

than the α_2 phase. Accordingly, the hot-rolled alloy thermally treated at 1200 °C, which is characterized with the higher volume fraction of the β phase in the microstructure, showed higher high-temperature oxidation resistance in the air.

2. Oxidation temperature and oxidation duration show considerable influence on the investigated alloy degradation process. During oxidation in air at 600 °C on the alloy surface, the compact single-layered scale was obtained and its detachment from the alloy surface was noticed only during the last stage of the cyclic oxidation process. On the other hand, during the cyclic oxidation at 900 °C the oxidation process was intensified and, as a result of the more intensive oxidation degradation process, on the alloy surface, the multi-layered scale was formed while cracking and detachment of the external scale fragments was noticed much earlier than in the case of oxidation at a lower temperature.
3. The main oxidation products are Al_2O_3 and TiO_2 particles. These oxides were present in the externally formed scales as individual layers or as mixed porous layers. The presence of Al_2O_3 particles is beneficial for the alloy oxidation resistance, while the presence of TiO_2 layers caused accelerated degradation of the alloy due to their porosity. The presence of pores in the TiO_2 layers enabled easier oxygen diffusion and thus resulted in faster alloy degradation. At the beginning of the cyclic oxidation process, thin Ti and Al nitride layers can also be formed.
4. Kinetic models were defined based on the mass gain *vs.* oxidation time results. These models confirmed that a more distinct oxidative degradation process is characteristic for the alloy hot-rolled at 1050 °C than for the hot-rolled alloy thermally treated at 1200 °C.
5. Oxidation rate constants, obtained during this study, confirmed that the oxidation process was significantly faster when it was performed at a higher temperature.
6. Linear progression of the mass gain with time is found to be characteristic for the oxidation at 600 °C of the hot-rolled alloy thermally treated at 1200 °C, while its oxidation at 900 °C can be described by the parabolic kinetic model.

Acknowledgments

This research was financially supported by the Ministry of Education, Science and Technological Development of the Republic of Serbia.

References

[1] Djanarthany, S., Viala, J.C., Bouix, J., An overview of monolithic titanium aluminides based on Ti_3Al and TiAl, *Materials Chemistry and Physics*, *72* (2001), 3, pp. 301-319

[2] Yang, H.S., Jin, P., Mukherjee, A.K., Superplastic behavior of regular α_2 and super α_2 titanium aluminides, in: *High Temperature Aluminides and Intermetallics* (Eds. S.H. Whang, C.T. Liu, D. Pope), TMS, Warrendale, PA, 1992, p. 457-464

[3] Li, Z., Gao, W., Yoshihara, M., He, Y., Improving oxidation resistance of Ti_3Al and TiAl intermetallic compounds with electro-spark deposit coatings, *Materials Science and Engineering: A*, *347* (2003), 1-2, pp. 243-252

[4] Froes, F.H., Suryanarayana, C., Eliezer, D., Synthesis, properties and applications of titanium aluminides, *Journal of Materials Science*, *27* (1992), pp. 5113-5140

[5] Austin, C.M., Current status of gamma Ti aluminides for aerospace applications, *Current Opinion in Solid State and Materials Science*, *4* (1999), 3, pp. 239-242

[6] Loria, E.A., Gamma titanium aluminides as prospective structural materials, *Intermetallics*, *8* (2000), pp. 1339-1345

[7] Bania, P.J., An Advanced Alloy for Elevated Temperatures, *JOM*, *40* (1988), 3, pp. 20-22

[8] Lipsitt, H.A., Titanium Aluminides - An Overview, in: *High-Temperature Ordered Intermetallic Alloys, vol. 39* (Eds. C.C. Koch, C.T. Liu, N.S. Stoloff), Materials Research Society, Pittsburgh, PA, 1985, pp. 351-364

[9] Blackburn, M.J., Smith, M.P., Research to Conduct an Exploratory Experimental and Analytical Investigation of Alloys, U.S. Air Force Wright Aeronautical Laboratories, Technical Report No. AFWAL-TR-80-4175, 1980

[10] Blackburn, M.J., Smith, M.P., R&D on Composition and Processing of Titanium Aluminide Alloys for Turbine Engine, U.S. Air Force Wright Aeronautical Laboratories, Technical Report No. AFWAL-TR-82-4086, 1982
[11] Smith, M., Huang, S.C., Broderick, T.F., private communication with author, P&W, GE-Schenectady, WRDC, 1989
[12] Schafrik, R.E., Dynamic elastic moduli of the titanium aluminides, *Metallurgical Transactions A*, 8 (1977), pp. 1003-1006
[13] Lipsitt, H.A., Advanced High Temperature Alloys: Processing and Properties, in: *Advanced High-Temperature Alloys: Processing and Properties* (Eds. S.M. Allen, R.M. Pelloux, R. Widmer), ASM, Metals Park, Ohio, 1986, pp. 157-165
[14] Choudhury, N.S., Graham, H.C., Hinze, J.W., *Properties of High Temperature Alloys with Emphasis on Environmental Effects*, Electrochemical Society, Pennington, New York, 1976
[15] Schaeffer, J.C., Isothermal oxidation behavior of alpha-2 titanium aluminide alloys, Scripta Metallurgica et Materialia, *28* (1993), 7, pp. 791-796
[16] Subrahmanyam, J., Cyclic oxidation of aluminized Ti-14Al-24Nb alloy, *Journal of Materials Science*, *23* (1988), pp. 1906-1910
[17] Nishimoto, T., Izumi, T., Hayashi S., Narita, T., Effect of coating layer structures and surface treatment on the oxidation behavior of a Ti-50 at.%Al alloy, *Intermetallics*, *11* (2003), pp. 459-466
[18] Li, Z., Gao, W., He, Y., Protection of a Ti_3Al-Nb alloy by electro-spark deposition coating, *Scripta Materialia*, 45 (2001), 9, pp. 1099-1105
[19] Khobaib, M., Vahldiek, F.W., High temperature oxidation behavior of Ti_3Al alloys, in: *Space Age Metals Technology, vol. 2* (Eds. F.H. Froes, R.A. Cull), SAMPE, Covina, CA, 1988, pp. 262-270
[20] Meier, G.H., Pettit, F.S., The oxidation behavior of intermetallic compounds, in: *High Temperature Aluminides and Intermetallics* (Eds. S.H. Whang, C.T. Liu, D. Pope), TMS, Warrendale, PA, 1992, pp. 548-560
[21] Yang, K.L., Huang, J.C., Wang, Y.N., Phase transformation in the β phase of super α_2 Ti_3Al base alloys during static annealing and superplastic deformation at 700-1000 °C, *Acta Materialia*, *51* (2003) 9, pp. 2577-2594
[22] Cvijović, I., Cyclic oxidation of the Ti_3Al-based intermetallic alloy (in Serbian), M.Sc. thesis, University of Belgrade, Belgrade, Serbia, 2006
[23] Tomasi, A., Gialanella, S., Oxidation phenomena in a Ti_3Al base-alloy, *Thermochemica Acta*, 269-270 (1995), pp. 133-143